The American Journal of Clinical Nutrition xxx (xxxx) xxx

The American Journal of CLINICAL NUTRITION

journal homepage: www.journals.elsevier.com/the-american-journal-of-clinical-nutrition

Original Research Article

Smartphone prediction of skeletal muscle mass: model development and validation in adults

Cassidy McCarthy [1], Grant M. Tinsley [2], Shengping Yang [1], Brian A. Irving [3], Michael C. Wong [4], Jonathan P. Bennett [4], John A. Shepherd [4], Steven B. Heymsfield [1,*]

[1] *Pennington Biomedical Research Center, Louisiana State University System, Baton Rouge, LA, United States;* [2] *Department of Kinesiology and Sport Management, Texas Tech University, Lubbock, TX, United States;* [3] *School of Kinesiology, Louisiana State University, Baton Rouge, LA, United States;* [4] *University of Hawaii Cancer Center, Honolulu, HI, United States*

A B S T R A C T

Background: Skeletal muscle is a large and clinically relevant body component that has been difficult and impractical to quantify outside of specialized facilities. Advances in smartphone technology now provide the opportunity to quantify multiple body surface dimensions such as circumferences, lengths, surface areas, and volumes.

Objectives: This study aimed to test the hypothesis that anthropometric body measurements acquired with a smartphone application can be used to accurately estimate an adult's level of muscularity.

Methods: Appendicular lean mass (ALM) measured by DXA served as the reference for muscularity in a sample of 322 adults. Participants also had digital anthropometric dimensions (circumferences, lengths, and regional and total body surface areas and volumes) quantified with a 20-camera 3D imaging system. Least absolute shrinkage and selection operator (LASSO) regression procedures were used to develop the ALM prediction equations in a portion of the sample, and these models were tested in the remainder of the sample. Then, the accuracy of the prediction models was cross-validated in a second independent sample of 53 adults who underwent ALM estimation by DXA and the same digital anthropometric estimates acquired with a smartphone application.

Results: LASSO models included multiple significant demographic and 3D digital anthropometric predictor variables. Evaluation of the models in the testing sample indicated respective RMSEs in women and men of 1.56 kg and 1.53 kg and R^2's of 0.74 and 0.90, respectively. Cross-validation of the LASSO models in the smartphone application group yielded RMSEs in women and men of 1.78 kg and 1.50 kg and R^2's of 0.79 and 0.95; no significant differences or bias between measured and predicted ALM values were observed.

Conclusions: Smartphone image capture capabilities combined with device software applications can now provide accurate renditions of the adult muscularity phenotype outside of specialized laboratory facilities. *Am J Clin Nutr* 2023;x:xx.

This trial was registered at clinicaltrials.gov as NCT03637855 (https://clinicaltrials.gov/ct2/show/NCT03637855), NCT05217524 (https://clinicaltrials.gov/ct2/show/NCT05217524), and NCT03771417 (https://clinicaltrials.gov/ct2/show/NCT03771417).

Keywords: optical imaging, body composition, nutritional assessment, malnutrition, obesity, sarcopenia

Introduction

Skeletal muscle is the largest body component in most adults [1], with adipose tissue being a major determinant of a person's shape [2]. Jindřich Matiegka, the Czech anthropologist, recognized these associations in 1921 when he first reported an anthropometric method of quantifying whole-body skeletal muscle mass that applied measured values for body circumferences, skinfolds, and height [3]. Matiegka models were developed using information on skeletal muscle mass proportions obtained from human cadavers. The development of noninvasive reference methods for quantifying skeletal muscle mass in vivo during the 1970s and 1980s [4], such as computed tomography, MRI, and DXA, led to further development of anthropometric approaches for predicting a person's muscle mass [5–9]. These reference methods were used to estimate regional or whole-body skeletal muscle mass that were set as dependent variables in anthropometric prediction

Abbreviations used: 3D, three-dimensional; ALM, appendicular lean mass; LASSO, Least Absolute Shrinkage and Selection Operator; PBRC, Pennington Biomedical Research Center; TOST, two 1-sided test; UHCC, University of Hawaii Cancer Center.

* Corresponding author.
E-mail address: steven.heymsfield@pbrc.edu (S.B. Heymsfield).

https://doi.org/10.1016/j.ajcnut.2023.02.003
Received 11 August 2022; Received in revised form 18 January 2023; Accepted 2 February 2023; Available online xxxx

models. Predictor variables in these models typically included race/-ethnicity, sex, age, weight, height, and multiple body circumferences [5–9].

The recent introduction and refinement of 3-dimensional (3D) optical imaging methods has stimulated new interest in digital anthropometric prediction of body components such as total body fat mass [2, 10–12]. Whole-body optical imaging system costs continue to decline, whereas the accuracy of circumference, length, surface area, and volume estimates improves [13–15]. The wave of new imaging devices includes smartphones coupled with applications that use artificial intelligence and machine learning to process two-dimensional (2D) captured images to 3D avatars that accurately portray multiple anthropometric dimensions that can be used to quantify body size and shape [16–18].

These recent developments led us to hypothesize that body dimensions acquired with a smartphone can be used to estimate an adult's level of muscularity. The aim of the current proof-of-concept study was to test this hypothesis by first developing and then testing digital anthropometric skeletal muscle mass prediction equations in a sample of healthy adults using a validated 20-camera 3D optical scanning system to acquire multiple measures of body size and shape. Then, the predictive value of these equations was cross-validated in a new independent sample of adults using a smartphone application that digitally estimates the same anthropometric body dimensions as the 20-camera system.

Methods

Study design and participants

Skeletal muscle mass prediction equations were developed and tested in a sample of healthy adults recruited at two sites, Pennington Biomedical Research Center (PBRC) in Baton Rouge, LA, and at the University of Hawaii Cancer Center (UHCC) in Honolulu, HI. This phase of the investigation was part of the "Shape Up! Adults" study that was approved by the institutional review boards of PBRC and UHCC; all participants provided informed consent. The recruitment methods and inclusion/exclusion criteria for this study are reported in previous publications [2,19,20] and in Supplemental Figure 1. Appendicular lean mass (ALM) measured by DXA was used as a surrogate reference estimate of whole-body skeletal muscle mass as previously reported [21]. Whole-body 3D scans using a 20-camera optical imaging system (SS20, software version 6.2.1.; Size Stream) captured key body circumferences, lengths, surface areas, and volumes. The term "circumference" as applied in this study is synonymous with the more commonly used term "girth" in the anthropology literature. ALM prediction models were developed and tested as described in the Statistical Methods section.

The ALM prediction equations developed in the SS20 group were cross-validated in a second independent sample of healthy adult participants at PBRC. This smartphone phase of the study was approved by the center's institutional review board, and all participants signed the approved informed consent. These participants were part of a larger 2-institution study during which the relevant measurements were made only at the PBRC site (Supplemental Figure 1). ALM was measured with DXA in each participant who also completed a smartphone scan with a free downloadable application [MeThreeSixty (Me360), software version 3.4.1.; Size Stream] [17]. The application was used to collect the same digital anthropometric data set as with the SS20 scanner in the equation development and testing phase of the study. Earlier studies from our group reported comparable digital anthropometric circumference measurements across SS20 and Me360 systems that also agreed favorably with flexible tape measurements made by a trained technician [17]. The predictive value of the ALM equations was evaluated in the Me360 group as described in the Statistical Methods section.

Measurements

The single study visit included measurement of participant body weight (±0.1 kg; PBRC/UHCC: B-Tek Scales; Seca 284; Seca) and height (±0.1 cm; Seca 222; Seca 284). The participants were clothed in undergarments and a gown provided by both centers. Two weight and height measurements were acquired and averaged; a third measurement was taken when there were respective discrepancies of >0.5 kg and >0.5 cm.

3D scans

Attire for the 3D scans included hair coverage with a spandex cap and spandex shorts and, for women, a sports bra. Participants were scanned two times on the SS20 and measurements averaged; a third scan was completed when large measurement discrepancies were present. The SS20 Classic Edition is a stationary whole-body 3D optical scanner. The SS20 scanner has 20 infrared depth sensors that are mounted on four corners of a rectangular aluminum frame. The participant holds height-adjusted handlebars while standing on footprint guides at the device's center. Feet are held shoulder-width apart and participant arms extended downward at a 45° angle from each side of the body. The 20 infrared projectors transmit a structured light pattern onto participants, and distortions in the light pattern generated by the person's 3D shape are recorded during the 6-s scan by cameras and used to calculate depth.

The Me360 smartphone application was housed on an iPhone X (Apple). The smartphone application required entry of the participant's age, height, and weight. Then, voice prompts from the application navigated the participant into the "A-pose" position, similar to that for the SS20, for the self-administered scan; verbal commands adjusted the participant's pose as required to secure a proper image. In addition, images of the participant's front and side were acquired. Duplicate images were averaged; a third scan was collected if there were large measurement discrepancies between the first two. The application's software generated a deidentified 3D avatar that included anthropometric measurements. The .obj image files and associated .csv anthropometric data files were downloaded and used in validating the skeletal muscle mass prediction models.

The CV, expressed in %, for both scanners were similar and, for example, ~1.0% for waist and hip circumferences and 1.5%–2.5% for extremity circumferences (Supplemental Table 1) [17].

DXA

Each participant completed a DXA scan for measurement of total body and regional fat mass, lean mass, and bone mineral content. Duplicate scans were completed on participants and the measured values averaged. DXA scans were conducted according to manufacturer's guidelines either with a Hologic Discovery A or Horizon A system (Hologic). Both DXA scanners were calibrated according to standard Hologic procedures [22], and DXA cross-calibration phantoms were scanned at the PBRC and UHCC sites. The DXA scans were

analyzed by a trained technician using Hologic Apex software version 5.6 (Hologic) with the National Health and Nutrition Examination Survey option disabled. Fat, lean mass, and bone mineral content have respective between-measurement CVs of 1.0%, 0.5%, and 0.5% as reported earlier [23]. The ALM was calculated as the sum of each extremity's lean mass. The respective CVs for ALM, leg lean mass, and arm lean mass are 0.85%, 1.01%, and 1.54%, respectively (Supplemental Table 1).

Statistical methods

Model development

Least Absolute Shrinkage and Selection Operator (LASSO) regression procedures were used to develop the ALM (skeletal muscle) prediction equations. Demographic and anthropometric variables from the SS20 3D optical scans were used to predict DXA-derived ALM, adjusted for measurement site. Models were fit using the following predictor variables: age, race/ethnicity, height, and weight; circumferences of the chest, neck, head, hips, waist, ankle, upper arm, forearm, and thigh; lengths of the arms and legs; surface areas of the whole body, torso, arms, and legs; and volumes of the whole body, torso, arms, and legs. Circumferences and lengths were averages of the values for the left and right sides of the body, when applicable. Surface areas and volumes were sums of the left and right sides of the body, when applicable. For each model, a training data set of 80% of the sample and a testing data set of 20% of the sample were produced using random sampling procedures in R (v 4.1.2) [24]. LASSO regression procedures were performed to fit models, using the *glmnet* R package [25]. LASSO regression uses constraints on model parameters that shrink coefficients toward zero [25,26]. Shrinkage to zero excludes unnecessary predictor variables from the model (that is, model selection) and encourages sparse models. These models identify the variables and coefficients that minimize model prediction error and emphasize the best combined prediction of the outcome rather than a focus on interpretations regarding contributions of individual variables [27]. The λ value informs the shrinkage procedures to limit the complexity of the model. Using 10-fold crossvalidation, the ideal λ value using the one SE rule was identified and selected for use in model development (that is, the λ value that gives the most regularized model such that cross-validated error is within one SE of the minimum).

Using the testing data set, performance of the developed models was evaluated through the root mean squared error (RMSE), coefficient of determination (R^2), Bland-Altman analysis, equivalence testing, and null hypothesis significance testing (paired *t* tests). For equivalence testing, an equivalence interval of ±1.0 kg ALM was used for the two one-sided tests (TOST) [28]. These analyses were performed using the *DescTools* [29], *TOSTER* [30], and *ggplot2* [31] R packages. The same procedures were performed with the independent cross-validation smartphone sample that had paired DXA and Me360 3D optical variables. Statistical significance was accepted at $P < 0.05$.

Results

Participants

The SS20 model development and testing sample included 322 adults: 178 women and 144 men (Table 1 and Supplemental Figure 1). The group average age was ~45 y with a body mass index of ~27–28 kg/m^2. The training data set included 257 of the 322 adults, and the testing sample included the remaining 65 adults. The Me360 smartphone sample included 53 adults (27 women and 26 men) with an average age of ~39 y and a body mass index of ~29 kg/m^2. The mean group values for SS20 and Me360 anthropometric dimensions are summarized in Table 1. Both samples were heterogeneous for self-reported race and ethnicity (Supplemental Table 2).

TABLE 1
Participant Characteristics (mean ± SD)

Sample	SS20		Me360	
	Women	Men	Women	Men
N	178	144	27	26
Age (y)	47.3 ± 17.6	45.0 ± 17.0	38.6 ± 15.3	39.0 ± 14.1
Height (cm)	162.0 ± 6.7	175.0 ± 6.3	163.7 ± 7.1	176.4 ± 7.9
Weight (kg)	69.6 ± 16.5	87.2 ± 17.6	78.3 ± 22.8	91.4 ± ± 25.8
BMI (kg/m^2)	26.5 ± 6.1	28.4 ± 5.5	29.3 ± 8.4	29.2 ± 7.8
ALM (kg)	17.5 ± 3.4	27.3 ± 4.6	19.4 ± 3.9	28.2 ± 6.5
Head circumference (cm)	56.9 ± 3.9	57.6 ± 2.6	61.9 ± 2.8	59.7 ± 2.9
Collar circumference (cm)	34.7 ± 3.9	40.9 ± 4.4	36.1 ± 3.4	41.4 ± 3.8
Chest circumference (cm)	96.0 ± 13.6	107.3 ± 12.6	106.7 ± 17.4	113.1 ± 15.9
Forearm circumference (cm)	25.8 ± 2.9	29.9 ± 3.0	26.3 ± 3.0	29.5 ± 3.2
Upper arm circumference (cm)	33.2 ± 4.6	36.5 ± 4.4	33.8 ± 5.6	36.6 ± 5.5
Waist circumference (cm)	96.3 ± 14.4	96.2 ± 12.9	103.2 ± 17.7	99.1 ± 16.0
Hip circumference (cm)	106.8 ± 11.5	106.5 ± 11.1	113.9 ± 14.2	110.3 ± 13.1
Thigh circumference (cm)	58.2 ± 6.7	58.8 ± 6.3	63.1 ± 8.8	61.4 ± 7.9
Ankle circumference (cm)	22.8 ± 1.9	24.2 ± 2.0	24.0 ± 1.7	25.0 ± 1.6
Arm length (cm)	55.4 ± 3.1	59.6 ± 3.3	56.5 ± 3.4	60.9 ± 3.5
Outside leg length (cm)	99.9 ± 5.9	104.6 ± 6.0	102.1 ± 4.7	105.7 ± 5.5
Surface area arm (cm^2)	2979 ± 359	3604 ± 418	3130 ± 422	3744 ± 565
Surface area torso (cm^2)	5878 ± 815	6824 ± 854	6443 ± 1046	7104 ± 1190
Surface area leg (cm^2)	8103 ± 809	8791 ± 822	8967 ± 1176	9393 ± 1207
Surface area total (cm^2)	16,961 ± 1785	19,220 ± 1896	18,533 ± 2560	20,218 ± 2839
Arm volume (cm^3)	7170 ± 1446	9544 ± 1888	9104 ± 2173	11,222 ± 2785
Torso volume (cm^3)	47,015 ± 12,910	57,800 ± 14,155	54,491 ± 16,967	62,640 ± 18,973
Leg volume (cm^3)	17,252 ± 3577	18,782 ± 3389	20,377 ± 5184	20,704 ± 5262
Total volume (cm^3)	71,479 ± 16,815	86,182 ± 18,127	83,834 ± 23,624	94,794 ± 25,760

Values are given as mean ± SD. ALM, appendicular lean mass; Me360, MeThreeSixty.

Model development

The predictor variables retained in the LASSO regression models were as follows: for women—age, height, weight, and race/ethnicity (all except Asian); circumferences of the neck, head, waist, ankle, forearm, and upper arm; leg length; and surface area of the legs; and for men—height, weight, and race/ethnicity (Native Hawaiian and other Pacific Islander; other race groups NS); circumferences of the chest, head, waist, forearm, and thigh; leg lengths; surface area of the arms; and volumes of the torso, legs, and arms. For each model, the coefficients of the remaining variables were shrunk to zero, equivalent to removal from the model. Model coefficients are displayed in Table 2. For women and men, the model R^2 and mean cross-validated error were 0.83 and 2.69 ± 0.28 kg (mean ± SE) and 0.91 and 2.63 ± 0.14 kg, respectively.

Model evaluation

For women, evaluation of the LASSO model in the SS20 testing data set indicated an RMSE of 1.56 kg and R^2 of 0.74 (Figure 1A). A comparison between measured (DXA) and predicted ALM values indicated equivalence between methods (TOST CI: −0.54, 0.35 kg; $P = 0.0008$) and no significant difference between methods using paired t test ($P = 0.71$). The Bland-Altman analysis indicated a slight proportional bias between measured and predicted values (Figure 1B) (slope 95% CI: −0.40, −0.03). In addition, a difference from the line of identity was observed for the slope (95% CI: 0.56, 0.85) and intercept (95% CI: 2.46, 7.56). In the separate cross-validation sample using the Me360 application, an RMSE of 1.78 kg and R^2 of 0.79 were observed (Figure 1C). A comparison between DXA and predicted ALM values indicated equivalence between methods (TOST CI: −0.77, 0.42 kg; $P = 0.01$) and no significant difference between methods using paired t test ($P = 0.62$). In addition, the Bland-Altman analysis indicated no significant proportional bias between measured and predicted values (Figure 1D) (slope 95% CI: −0.24, 0.16). Furthermore, no differences from the line of identity were observed for the slope (95% CI: 0.68, 1.04) and intercept (95% CI: −1.03, 6.11).

For men, evaluation of the LASSO model in the SS20 testing data set indicated an RMSE of 1.53 kg and R^2 of 0.90 (Figure 2A). A comparison between DXA and predicted ALM values indicated equivalence between methods (TOST CI: −0.60, 0.38 kg; $P = 0.002$) and no significant difference between methods using paired t test ($P = 0.70$). In addition, the Bland-Altman analysis indicated no significant proportional bias between measured and predicted values (Figure 2B) (slope 95% CI: −0.23, 0.03). However, a difference from the line of identity was observed for the slope (95% CI: 0.74, 0.97) and intercept (95% CI: 0.65, 7.02). In the separate cross-validation sample using the Me360 data, an RMSE of 1.50 kg and R^2 of 0.95 were observed (Figure 2B). A comparison between DXA and predicted ALM values indicated equivalence between methods (TOST CI: −0.13, 0.87 kg; $P = 0.02$) and no significant difference between methods using paired t test ($P = 0.22$). Moreover, the Bland-Altman analysis indicated no significant proportional bias between measured and predicted values (Figure 2D) (slope 95% CI: −0.10, 0.10). Furthermore, no differences from the line of identity were observed for the slope (95% CI: 0.88, 1.07) and intercept (95% CI: −1.63, 3.87).

Discussion

Evaluations in this study confirmed our hypothesis that anthropometric surface dimensions acquired with a smartphone application can provide accurate estimates of a person's muscularity as defined by ALM. These evaluations progressed in three linked stages. First, we developed separate LASSO ALM prediction models for men and women that included a wide range of demographic and SS20-derived digital anthropometric covariates. The next step involved testing these models in a subgroup of the SS20 sample; R^2's were 0.74 and 0.90 with RMSEs of 1.56 kg and 1.53 kg in females and males, respectively. Then, the developed and tested SS20 ALM prediction models were cross-validated in a new independent sample with the Me360 smartphone application; R^2's were equally good at 0.79 and 0.95 with RMSEs of 1.78 kg and 1.50 kg in women and men, respectively. The resulting predicted and actual ALM values did not differ significantly, nor was a significant bias detected. Thus, the findings of this study strongly support the concept that reliable whole-body skeletal muscle mass estimates can be acquired in adults with a smartphone application. These observations are consistent with and extend earlier validation studies of key body circumference [17] and percentage body fat measurements with the Me360 smartphone application [32].

A consistent observation in this study was the greater ALM predictive value of equations developed in males than that in females. This finding is supported by the study of Al-Gindan et al. [5], who also found stronger relations between muscularity as quantified with MRI and flexible tape-measured body circumferences in males than those in females. This observation likely reflects greater between-individual differences in muscularity and, hence, anthropometric body dimensions among males than those in females [1]. In addition, females have a thicker subcutaneous adipose tissue layer covering underlying muscles that might further confound body surface measurements. The

TABLE 2
LASSO regression model coefficients for predicting ALM

	Women ($n = 142$)	Men ($n = 115$)
Intercept	−12.622	−27.386
Age (y)	−0.023	0
Race, Caucasian	−0.191	0
Race, Asian	0	0
Race, Black	0.427	0
Race, Hispanic	−0.288	0
Race, NHOPI	0.553	2.566
Race, Other	−0.709	0
Height (cm)	0.088	0.132
Weight (kg)	0.135	0.221
Head circumference (cm)	0.001	0.068
Collar circumference (cm)	0.019	0
Chest circumference (cm)	0	0.087
Forearm circumference (cm)	0.048	0.212
Upper arm circumference (cm)	0.078	0
Waist circumference (cm)	−0.039	−0.038
Hip circumference (cm)	0	0
Thigh circumference (cm)	0	0.020
Ankle circumference (cm)	0.083	0
Arm length (cm)	0	0
Outside leg length (cm)	0.023	−0.024
Surface area arm (cm^2)	0	0.0008
Surface area torso (cm^2)	0	0
Surface area leg (cm^2)	0.0003	0
Surface area total (cm^2)	0	0
Arm volume (cm^3)	0	0.00005
Torso volume (cm^3)	0	−0.0002
Leg volume (cm^3)	0	0.0003
Total volume (cm^3)	0	0

Race identification was self-reported. ALM, appendicular lean mass; NHOPI, Native Hawaiian and other Pacific Islander.

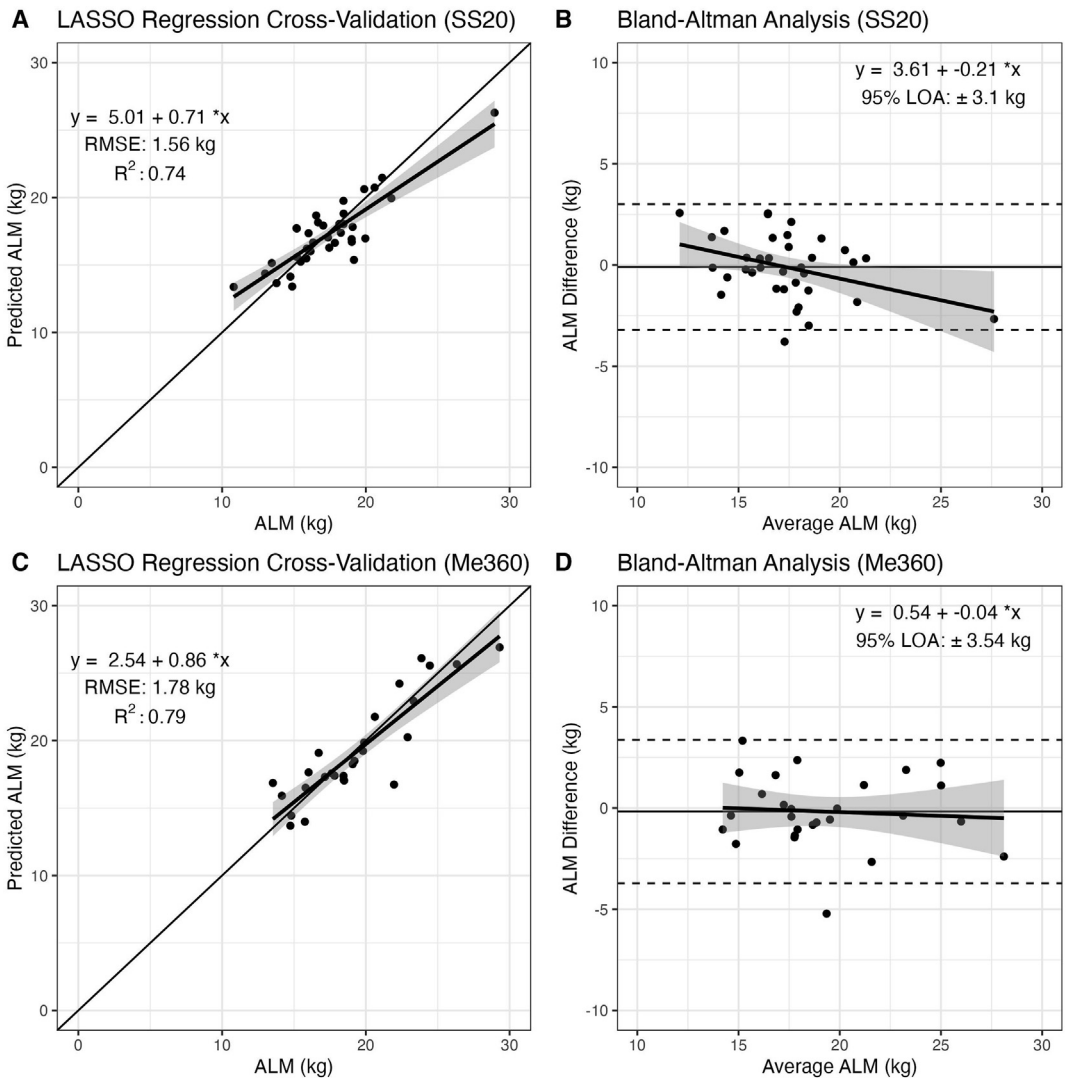

FIGURE 1. LASSO regression cross-validation and Bland-Altman analyses for the SS20 evaluations (A, B; $n = 36$) and the Me360 evaluations (C, D; $n = 27$) in women. The solid lines in panels A and C are the lines of identity and the regression lines with 95% CI (both, $P < 0.001$). In panels B and D, the solid horizontal line indicates the mean difference between DXA and predicted ALM, the dashed horizontal lines indicate the 95% limits of agreement (that is, 1.96 times the SD of the difference between DXA and predicted ALM), and the gray shading indicates the 95% CIs for the regression line. ALM, appendicular lean mass; LASSO, Least Absolute Shrinkage and Selection Operator; LOA, limits of agreement; Me360, MeThreeSixty.

observed limits of agreement were ~3 kg in both males and females, although relative to baseline ALM, the limits of agreement were larger in females (~11%) than those in males (~16%). Thus, although optical imaging methods are clearly of value in estimating group or population muscularity, accurate estimates in individuals remains open to future investigations.

This study also identified race/ethnicity covariates in developed ALM prediction models, as did Al-Gindan et al. [5] in their study. These kinds of observations, ones that need to be confirmed in larger race/ethnically heterogeneous samples, reveal the diversity of anatomic phenotypes that can be identified with newly emerging optical imaging devices that can rapidly and accurately quantify several hundred different body surface dimensions.

Despite their different technologies, size, and cost, both approaches yielded approximately similar measurement CVs and RMSEs for key body circumferences (Supplemental Table 1). The CVs increased inversely with region diameters with the values larger in the smaller arms than in the waist and hip. This observation likely portends less accurate arm muscle predictions than for the whole body and legs. The SS20 optical scanner has 20 depth cameras surrounding the participant that take simultaneous snapshots before reconstructing a 3D avatar. The Me360 smartphone application collects several 2D photographic silhouettes that are digitally extracted and associated with a 3D template mesh using artificial intelligence and machine learning algorithms. These Me360 data-processing steps culminate in a 3D replica of the person's scanned body. Avatars generated by both types of imaging approaches can be used to quantify body size and shape characteristics. Rapid technological advances are improving imaging devices, such as smartphone cameras and associated software. The possibility exists that soon digitally acquired anthropometric body dimensions will replace those obtained by skilled technologists as the reference in laboratory-based clinical trials.

The widely accepted LASSO method was used in this study to develop the ALM prediction equations [26,27]. Artificial intelligence and machine learning algorithms are also now being used with smartphone applications to predict body composition measures such as

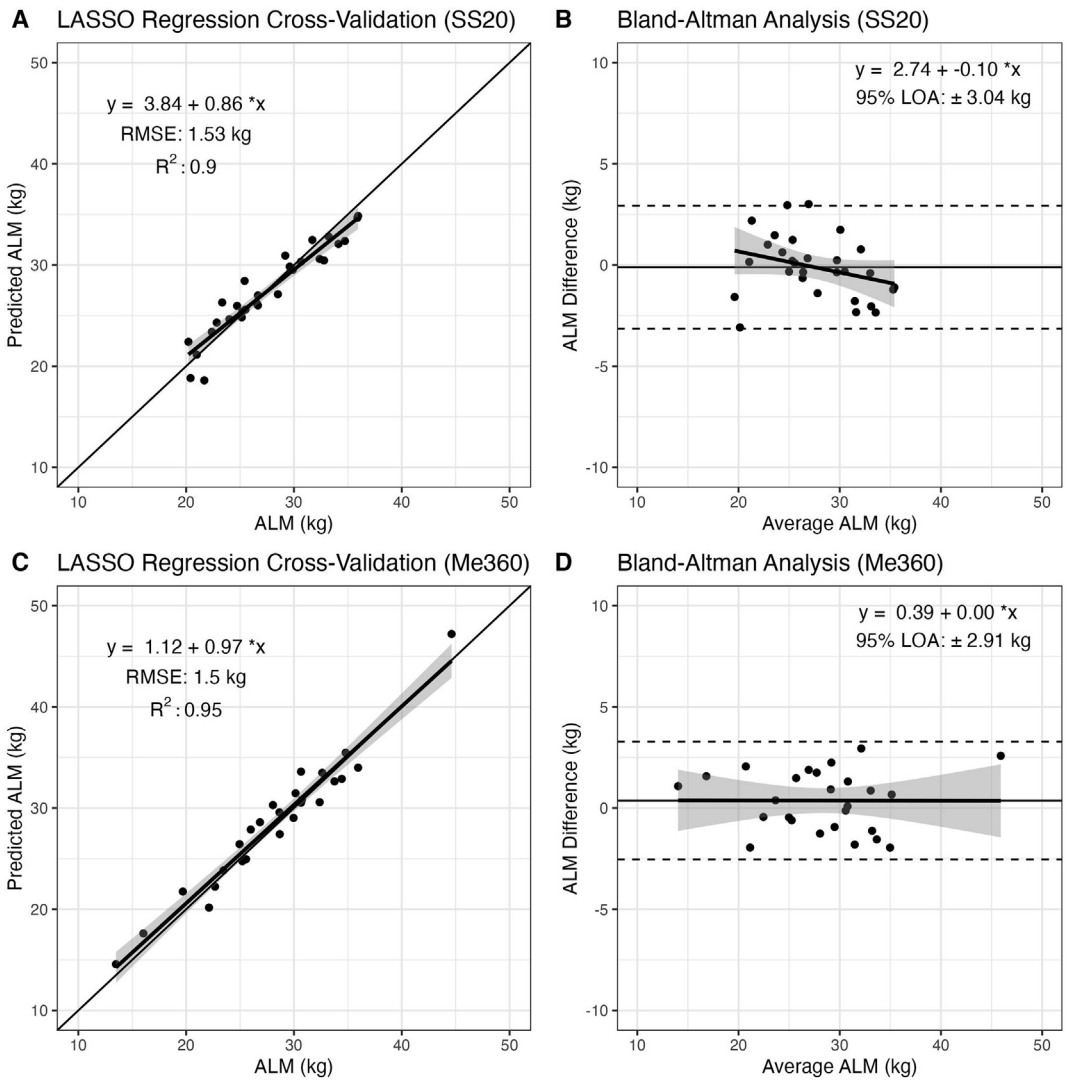

FIGURE 2. LASSO regression cross-validation and Bland-Altman analyses for the SS20 evaluations (A, B; $n = 29$) and the Me360 evaluations (C, D; $n = 26$) in men. The solid lines in panels A and C are the lines of identity and the regression lines with 95% CI (both, $P < 0.001$). In panels B and D, the solid horizontal line indicates the mean difference between DXA and predicted ALM, the dashed horizontal lines indicate the 95% limits of agreement (that is, 1.96 times the SD of the difference between DXA and predicted ALM), and the gray shading indicates the 95% CIs for the regression line. ALM, appendicular lean mass; LASSO, Least Absolute Shrinkage and Selection Operator; LOA, limits of agreement; Me360, MeThreeSixty.

fat percentage [11,32]. Future studies are needed to sort out the optimum statistical and mathematical approaches for developing prediction models such as the ones created in this study. These questions will be of increasing relevance as potential samples grow into the millions with 3D optical devices acquiring data on a global scale and housing this digital information in cloud-based sites [15,33]. A key consideration is that prediction model complexity is no longer a concern when equations are housed within a smartphone application or in cloud software.

This study has several limitations. First, our goal was to establish proof-of-concept for smartphone application potential as a means of quantifying total body skeletal muscle mass. Therefore, our developed ALM models are device and software version specific and are not generalizable beyond the SS20 and Me360 devices. Future studies with large and diverse samples can potentially use "universal" software [15,33] to process optical images acquired using any 3D imaging device and to generate standardized anthropometric dimensions and linked body composition prediction models. Second, we used DXA ALM as a proxy for total body skeletal muscle mass [21]. Use of computed tomography and MRI to quantify muscle mass in the future is increasingly feasible on a large scale with the introduction of automated software [34] that will reduce image-processing costs and be available outside of highly specialized facilities. Third, our focus was on "total" muscle mass and not on potentially accessible muscle groups such as in the arms and legs. Fourth, although our participants recorded stable weights over months and fasting at the time of evaluation, we did not control for factors that might influence body composition such as menstrual cycle activity, recent high sodium diets, and use of diuretics, factors that can add variability of measurements and predictions. Fifth, our participant measurements were made under laboratory conditions that included recommended participant attire and optimum lighting. Future studies in typical nonresearch settings are needed to establish the real-world accuracy of the methods described in this study. Finally, our validation samples for men and women were relatively small with <30 participants in each sex group in the Me360 evaluations. Larger samples will give a greater confidence in smartphone ALM prediction in future studies.

In conclusion, this study confirms that anthropometric body surface dimensions obtained with a smartphone application can be used to estimate an adult's level of muscularity. These observations lend further support to the view that rapid advances in digital technology, data-processing tools, and vast data storage capabilities will soon make deep body composition phenotyping capabilities widely accessible beyond specialized laboratory settings.

We acknowledge the support of Ms. Melanie Peterson in preparing this manuscript.

The authors' responsibilities were as follows—CM, JS, GMT, and SBH: designed the research; CM, BI, MCW, JPB, JAS, and SBH: conducted the research; JAS and SBH: provided essential materials; CM, GMT, SY, and SBH: analyzed the data; and all authors: wrote the article, had primary responsibility for final content, and read and approved the final version of the manuscript. SBH reports his role on the Medical Advisory Boards of Tanita Corporation, Amgen, and Medifast; he is also an Amazon Scholar. GMT has received in-kind support for his research laboratory, in the form of equipment loan or donation, from manufacturers of body composition assessment devices, including Size Stream LLC; Naked Labs Inc.; Prism Labs Inc.; RJL Systems; MuscleSound; and Biospace, Inc. The other authors and their close relatives and their professional associates have no financial interests in the study outcome, nor do they serve as an officer, director, member, owner, trustee, or employee of an organization with a financial interest in the outcome or as an expert witness, advisor, consultant, or public advocate on behalf of an organization with a financial interest in the study outcome.

Funding

This work was partially supported by National Institutes of Health NORC Center grants: P30DK072476, Pennington/Louisiana; P30DK040561, Harvard; R01DK109008, Shape UP! Adults; and R21AG058181, Resistance Exercise and Low-Intensity Physical Activity Breaks in Sedentary Time to Improve Muscle and Cardiometabolic Health.

Data Availability

Data described in this manuscript will be made available on request and approval by the investigators.

Appendix A. Supplementary data

Supplementary data to this article can be found online at https://doi.org/10.1016/j.ajcnut.2023.02.003.

References

[1] S.B. Heymsfield, B. Smith, E.A. Chung, K.L. Watts, M.C. Gonzalez, S. Yang, et al., Phenotypic differences between people varying in muscularity, J. Cachexia Sarcopenia Muscle. 13 (2) (2022) 1100–1112.
[2] B.K. Ng, M.J. Sommer, M.C. Wong, I. Pagano, Y. Nie, B. Fan, et al., Detailed 3-dimensional body shape features predict body composition, blood metabolites, and functional strength: the Shape UP! studies, Am. J. Clin. Nutr. 110 (6) (2019) 1316–1326.
[3] J. Matiegka, The testing of physical efficiency, Am. J. Phys. Anthropol. 4 (3) (1921) 223–230.
[4] S.B. Heymsfield, H.H. Hu, W. Shen, O. Carmichael, Emerging technologies and their applications in lipid compartment measurement, Trends Endocrinol. Metab. 26 (12) (2015) 688–698.
[5] Y.Y. Al-Gindan, C. Hankey, L. Govan, D. Gallagher, S.B. Heymsfield, M.E. Lean, Derivation and validation of simple equations to predict total muscle mass from simple anthropometric and demographic data, Am. J. Clin. Nutr. 100 (4) (2014) 1041–1051.
[6] M.C. Gonzalez, A. Mehrnezhad, N. Razaviarab, T.G. Barbosa-Silva, S.B. Heymsfield, Calf circumference: cutoff values from the NHANES 1999–2006, Am. J. Clin. Nutr. 113 (6) (2021) 1679–1687.
[7] S.B. Heymsfield, A. Stanley, A. Pietrobelli, M. Heo, Simple skeletal muscle mass estimation formulas: what we can learn from them, Front. Endocrinol (Lausanne). 11 (2020) 31.
[8] R.C. Lee, Z. Wang, M. Heo, R. Ross, I. Janssen, S.B. Heymsfield, Total-body skeletal muscle mass: development and cross-validation of anthropometric prediction models, Am. J. Clin. Nutr. 72 (3) (2000) 796–803.
[9] A.L. Quiterio, E.A. Carnero, A.M. Silva, B.C. Bright, L.B. Sardinha, Anthropometric models to predict appendicular lean soft tissue in adolescent athletes, Med. Sci. Sports Exerc. 41 (4) (2009) 828–836.
[10] J.P. Bennett, Y.E. Liu, B.K. Quon, N.N. Kelly, M.C. Wong, S.F. Kennedy, et al., Assessment of clinical measures of total and regional body composition from a commercial 3-dimensional optical body scanner, Clin. Nutr. 41 (1) (2022) 211–218.
[11] M.D. Majmudar, S. Chandra, K. Yakkala, S. Kennedy, A. Agrawal, M. Sippel, et al., Smartphone camera based assessment of adiposity: a validation study, NPJ Digit. Med. 5 (1) (2022) 79.
[12] M.C. Wong, B.K. Ng, S.F. Kennedy, P. Hwaung, E.Y. Liu, N.N. Kelly, et al., Children and adolescents' anthropometrics body composition from 3-D optical surface scans, Obesity (Silver Spring). 27 (11) (2019) 1738–1749.
[13] M.E. Dechenaud, S. Kennedy, S. Sobhiyeh, J. Shepherd, S.B. Heymsfield, Total body and regional surface area: quantification with low-cost three-dimensional optical imaging systems, Am. J. Phys. Anthropol. 175 (4) (2021) 865–875.
[14] G.M. Tinsley, M.L. Moore, J.R. Dellinger, B.T. Adamson, M.L. Benavides, Digital anthropometry via three-dimensional optical scanning: evaluation of four commercially available systems, Eur. J. Clin. Nutr. 74 (7) (2020) 1054–1064.
[15] S. Sobhiyeh, A. Dunkel, M. Dechenaud, A. Mehrnezhad, S. Kennedy, J. Shepherd, et al., Digital anthropometric volumes: toward the development and validation of a universal software, Med. Phys. 48 (7) (2021) 3654–3664.
[16] K. Bartol, D. Bojanic, T. Petkovic, T. Pribanic, A review of body measurement using 3D scanning, IEEE Access 9 (2021) 67281–67301.
[17] B. Smith, C. McCarthy C, M.E. Dechenaud, M.C. Wong, J. Shepherd, S.B. Heymsfield, Anthropometric evaluation of a 3D scanning mobile application, Obesity (Silver Spring). 30 (6) (2022) 1181–1188.
[18] I.Y. Tian, B.K. Ng, M.C. Wong, S. Kennedy, P. Hwaung, N. Kelly, et al., Predicting 3D body shape and body composition from conventional 2D photography, Med. Phys. 47 (12) (2020) 6232–6245.
[19] G. Maskarinec, Y.B. Shvetsov, M.C. Wong, A. Garber, K. Monroe, T.M. Ernst, et al., Subcutaneous and visceral fat assessment by DXA and MRI in older adults and children, Obesity (Silver Spring). 30 (4) (2022) 920–930.
[20] M.C. Wong, B.K. Ng, I. Tian, S. Sobhiyeh, I. Pagano, M. Dechenaud, et al., A pose-independent method for accurate and precise body composition from 3D optical scans, Obesity (Silver Spring). 29 (11) (2021) 1835–1847.
[21] J. Kim, Z. Wang, S.B. Heymsfield, R.N. Baumgartner, D. Gallagher, Total-body skeletal muscle mass: estimation by a new dual-energy X-ray absorptiometry method, Am. J. Clin. Nutr. 76 (2) (2002) 378–383.
[22] Y. Lu, A.K. Mathur, B.A. Blunt, C.C. Gluer, A.S. Will, T.P. Fuerst, et al., Dual X-ray absorptiometry quality control: comparison of visual examination and process-control charts, J. Bone Miner. Res. 11 (5) (1996) 626–637.
[23] M.P. Rothney, F.P. Martin, Y. Xia, M. Beaumont, C. Davis, D. Ergun, et al., Precision of GE Lunar iDXA for the measurement of total and regional body composition in nonobese adults, J. Clin. Densitom. 15 (4) (2012) 399–404.
[24] R Core Team. *R: A language and environment for statistical computing*, https://www.R-project.org/ (2022). Cited, 1/15/2023
[25] J.H. Friedman, T. Hastie, R. Tibshirani, Regularization paths for generalized linear models via coordinate descent, J. Stat. Softw. 33 (1) (2010) 1–22.
[26] R. Tibshirani, Regression shrinkage and selection via the Lasso, J. R. Stat. Soc., B: Stat. Methodol. 58 (1) (1996) 267–288.
[27] J. Ranstam, J.A. Cook, LASSO regression, Br. J. Surg. 105 (10) (2018) 1348.
[28] P.M. Dixon, P.F. Saint-Maurice, Y. Kim, P. Hibbing, Y. Bai, G.J. Welk, A primer on the use of equivalence testing for evaluating measurement agreement, Med. Sci. Sports Exerc. 50 (4) (2018) 837–845.
[29] Signorell, A. et al. *DescTools: Tools for Descriptive Statistics, version 0.99.46*, https://cran.r-project.org/web/packages/DescTools/index.html (2022). Cited 1/15/2023
[30] D. Lakens, Equivalence tests: a practical primer for t-tests, correlations, and meta-analyses, Soc. Psychol. Personal. Sci. 1 (2017) 1–8.
[31] H. Wickham, ggplot2: elegant graphics for data analysis [Internet], Springer-Verlag, New York, 2016 [date updated, date cited]. Available from: https://link.springer.com/book/10.1007/978-3-319-24277-4. Cited 1/15/23.

[32] P.S. Harty, B. Sieglinger, S.B. Heymsfield, J.A. Shepherd, D. Bruner, M.T. Stratton, et al., Novel body fat estimation using machine learning and 3-dimensional optical imaging, Eur. J. Clin. Nutr. 74 (5) (2020) 842–845.

[33] S. Sobhiyeh, S. Kennedy, A. Dunkel, M.E. Dechenaud, J.A. Weston, J. Shepherd, et al., Digital anthropometry for body circumference measurements: toward the development of universal three-dimensional optical system analysis software, Obes. Sci. Pract. 7 (1) (2021) 35–44.

[34] A. Karlsson, J. Rosander, T. Romu, J. Tallberg, A. Grönqvist, M. Borga, et al., Automatic and quantitative assessment of regional muscle volume by multi-atlas segmentation using whole-body water-fat MRI, J. Magn. Reson. Imaging. 41 (6) (2015) 1558–1569.